Report on simulation of memristor physics

Alfred Ajay Aureate .R
EE10B052
EE Dept., IIT Madras

September 22, 2014

1 Introduction:

In 2008, HP labs came up with a phenomenological model of the missing fourth fundamental passive circuit element, memristor[1], as predicted by Leon Chua in 1971[2]. He predicted that such a device would have unique i-v characteristics, which would look like a pinched hysteresis loop, where current goes to zero, when voltage goes to zero. Thus, it is a passive circuit element, i.e. it does not generate or retain voltage. But, since memristance[1] (of the memristor made by HP labs),

$$M(q) = R_{OFF}\left(1 - \frac{\mu_v R_{ON}}{D^2} q(t)\right)$$

depends on charge at an instance, it means that the memristance is dependent on the previous history of the current (because charge is total current till that point), hence the name. The memristive systems in general[3], satisfy the following equations: $v = R(w,i)\,i$; and $\frac{dw}{dt} = f(w,i)$, in which v is the voltage, i the current, R the instantaneous resistance, and w is a state variable, and for "pure" memristors neither R nor f are explicit functions of i.

The memristor that HP labs came up with in 2008, had TiO_2layer between two layers of metal electrodes. Here stoichiometric TiO_2 is used, which is self-doped, i.e. it is actually, TiO_{2-x}. So, there are charged vacant oxygen sites and mobile oxygen ions. This region is divided into two, based on the doping - highly doped ON region and undoped OFF region. These regions have different resistances, and the memristor device experiences the combined effect, due to both. The physical model of this memristor is simulated here[4], where the middle layer is modeled as a combination of an highly doped semiconductor and the undoped material. The state variable, w corresponds to the position of the sharp dividing line between the doped and undoped semiconductor, and is bounded between two limits, 0 and L, that corresponds to the positions of the metal contacts at either side of a semiconductor film.

2 Model:

A 1D model of the device is considered, with a semiconductor thin film that contains charged mobile n-type dopants with a concentration distribution $N_D(x)$ confined by electrodes at $x = 0$ and $x = L$. The dimensions of the device along the $y-$ and $z-$directions are assumed to be much larger than L, which is a reasonable approximation for thin film structures. The active layer is partially compensated by a small amount of immobile and uniformly distributed p-type dopants with concentration $N_A \leq N_D^*$, the average concentration of mobile dopants ($N_D^* = \int (N_D(x)/L)\,dx$).

In the discussion that follows, all quantities that are explicitly denoted as functions of x are also functions of time and will be examined after certain time intervals have elapsed. For simplicity $N_D^* = 5 \times 10^{19} cm^{-3}$, I'll assume that both donors and acceptors are shallow, and thus their energy levels coincide with the corresponding conduction E_C and valence E_V band edges. In this case, one can neglect thermal generation and recombination currents for relatively large band gap materials. Here, $n(x)$ - electron concentration and $p(x)$ - hole concentration are approximated with Fermi-Dirac statistics, that is, with the separate quasi-Fermi potentials $\phi_n(x)$ and $\phi_p(x)$, respectively. Thus, the steady-state currents from the drift-diffusion approximation for electrons and holes are determined from

$$\nabla.(-en(x)\,\mu_n \nabla\phi_n(x)) = 0 \tag{1}$$

and

$$\nabla.(ep(x)\,\mu_p \nabla\phi_p(x)) = 0 \tag{2}$$

where $n(x) = n_i exp\left[\frac{q\phi_n(x)}{k_B T}\right]$ holds for electrons and similarly, for holes, I have $p(x) = n_i exp\left[-\frac{q\phi_p(x)}{k_B T}\right]$ while the Poisson equation for the active layer with uniform permittivity $\varepsilon\varepsilon_0$ is

$$-\varepsilon\varepsilon_0 \triangle\phi(x) = e\left(p(x) - n(x) + f_D(x) N_D(x) - f_A(x) N_A\right) \tag{3}$$

Here, e is the unit charge, $\phi(x)$ the electrostatic potential, and $\mu_n(\mu_p)$ is the electron (hole) mobility, which is assumed to be independent of the field. $f_D(x)$ and $f_A(x)$ are ionization factors for donors and acceptors, correspondingly, which are found from the population statistics and typically equal to unity for the considered simulation parameters.

The non-equilibrium mobile ion distribution and ion flux $J_{ION}(x)$ can also be found from drift-diffusion theory (here I am neglecting nonlinear drift in high electric fields) and the continuity equation, that is, for singly charged positive ions,

$$J_{ION}(x) = -eD_i \nabla N_D(x) - eN_D(x)\mu_i \nabla\phi(x) \tag{4}$$

and

$$\frac{e\partial N_D(x)}{\partial t} = -\nabla . J_{ION}(x) \tag{5}$$

where D_i and μ_i are the ion diffusion constant and mobility, respectively, which are related via the Einstein–Nernst equation.

In this study I'll consider only bulk-limited transport, and the interfaces are assumed to be purely ohmic for electrons. This, for example, might correspond to either metal electrodes with adjacent $\triangle$-doped semiconductor interfacial layers or heavily doped semiconductor electrodes with a band gap similar to that of the transport layer. The electron and hole concentrations are fixed to their equilibrium levels defined by the Fermi potential at the interface, such that for an applied bias v the boundary conditions are

$$\phi_n(0) = \phi_p(0) \tag{6}$$

and

$$\phi_n(L) = \phi_p(L) = \phi_n(0) + v \tag{7}$$

The interfaces are assumed to be trap free and completely blocking for mobile ions, so that the total number of mobile dopants, LN_D^* is constant, that is,

$$J_{ION}(0) = J_{ION}(L) = 0 \tag{8}$$

In this simulation, I'll neglect Joule heating and explicit temperature effects.

3 Simulation:

Equations 1–5 with boundary conditions 6–8 are solved numerically using an iterative procedure to achieve self-consistency.

3.1 Step 1:

Equation 1 has only one unknown, $\phi_n(x)/v_0$, because even $n(x)$ could be described in terms of $\phi_n(x)$. When written in discrete form, I have $\phi_n(x)$ in terms of $\phi_n(x+h)$ and $\phi_n(x-h)$, where h is the step size for distance in the simulation. I used the boundary conditions for $\phi_n(x)$ at the end points from equations 6 and 7, to get the values of $\phi_n(x)$ for all x. Then, similarly, I repeated the same things for holes using equation 2 and boundary conditions from equations 6 and 7, to get the values for $\phi_p(x)$ for all x. Actually, the exact finite difference form of equation 1 and 2 that I solved is derived as follows:

$$(1) \Rightarrow \nabla.(-en(x)\mu_n \nabla\phi_n(x)) = 0$$

we also know that,

$$n(x) = n_i exp\left[\frac{q\phi_n(x)}{k_B T}\right]$$

$$\Rightarrow -e\frac{\partial}{\partial x}\left[n_i exp\left(\frac{q\phi_n(x)}{k_B T}\right)\right]\mu_n \frac{\partial}{\partial x}(\phi_n(x)) - en_i exp\left(\frac{q\phi_n(x)}{k_B T}\right)\mu_n \frac{\partial^2}{\partial x^2}(\phi_n(x)) = 0$$

$$\Rightarrow \frac{q}{k_B T}\left[\frac{\partial}{\partial x}\left(\phi_n\left(x\right)\right)\right]^2 = -\frac{\partial^2}{\partial x^2}\left(\phi_n\left(x\right)\right)$$

where $\frac{k_B T}{q} = 26mV$. Now, this equation in finite difference form:

$$\frac{1}{0.026}\left[\frac{\phi_n\left(x+h\right)-\phi_n\left(x-h\right)}{2h}\right]^2 = -\frac{\phi_n\left(x+h\right)-2\phi_n\left(x\right)+\phi_n\left(x-h\right)}{h^2} \tag{9}$$

Now, similarly from equation 2 and $p\left(x\right) = n_i exp\left[\frac{-q\phi_p(x)}{k_B T}\right]$, I got the following difference equation for holes:

$$\frac{1}{0.026}\left[\frac{\phi_p\left(x+h\right)-\phi_p\left(x-h\right)}{2h}\right]^2 = \frac{\phi_p\left(x+h\right)-2\phi_p\left(x\right)+\phi_p\left(x-h\right)}{h^2} \tag{10}$$

By solving the above equations for $\phi_n\left(x\right)$ and$\phi_p\left(x\right)$, I got the following plot for electrons (figure 1) and holes (figure 2). Here, $v_0 =$ is input voltage and $N_D^* = 5 \times 10^{19} cm^{-3}$.

Figure 1: Quasi-fermi potential of electrons - $\phi_n(x)/v_0$

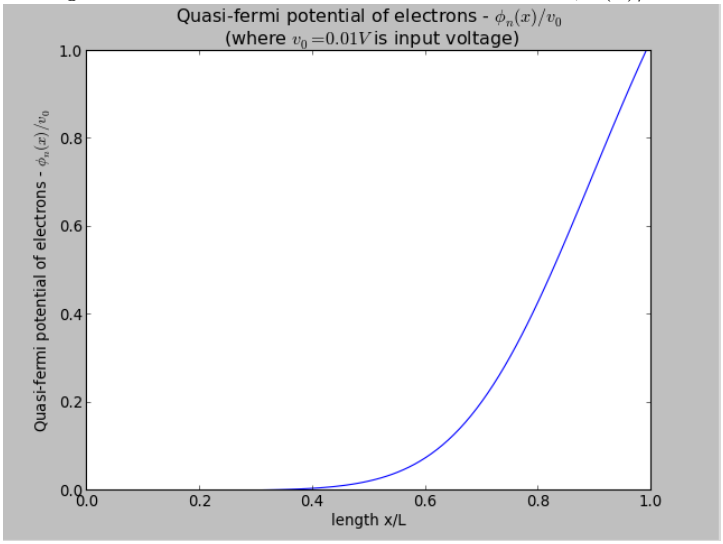

Figure 2: Quasi-fermi potential of holes - $\phi_p(x)/v_0$

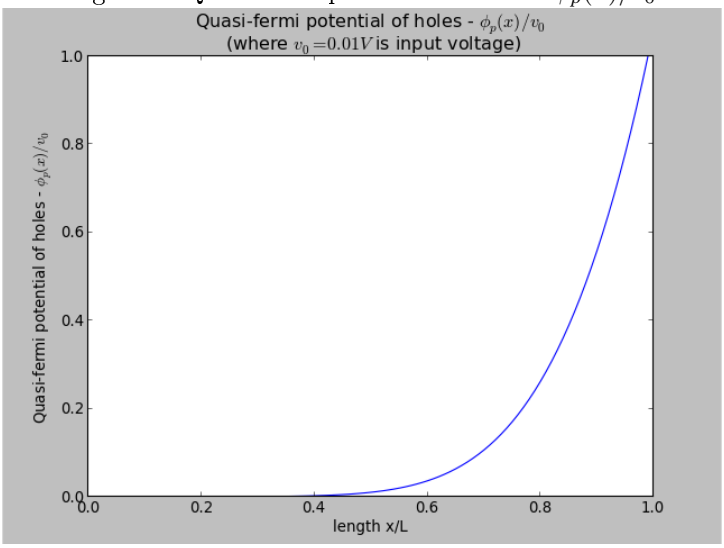

Figure 3: Mobile electron concentration - $n(x)/N_D^*$

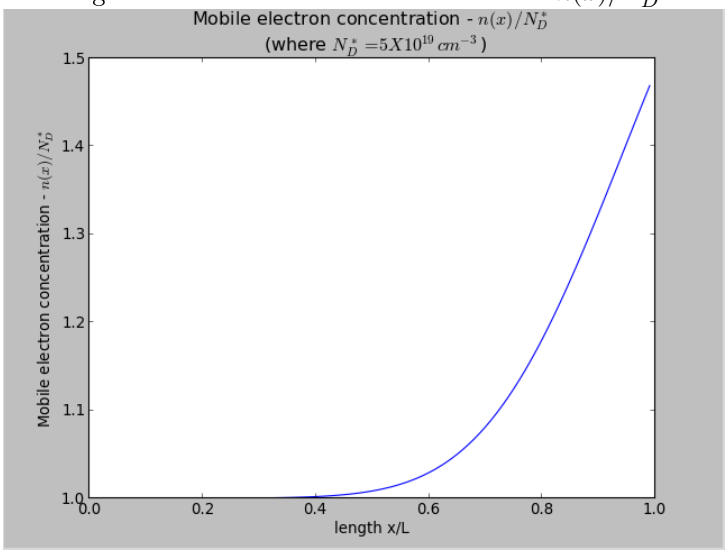

Figure 4: Mobile hole concentration - $p(x)/N_D^*$

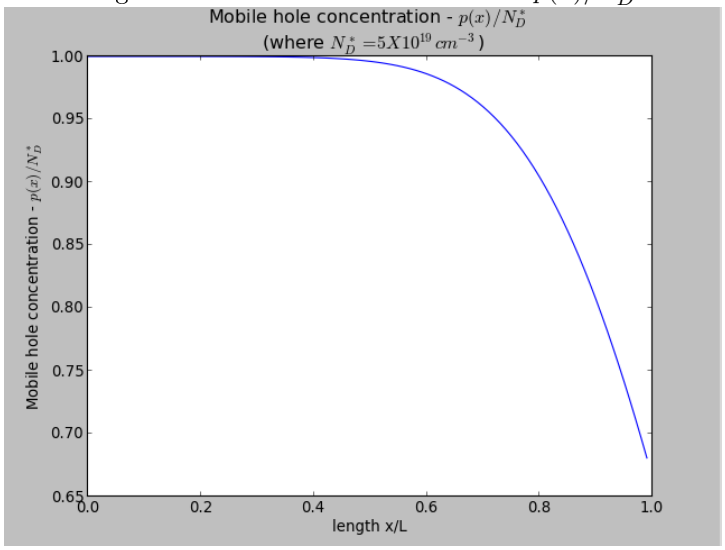

3.2 Step 2:

After this, I tried to solve for $\phi(x)$ from equation 3. Here, $n(x)$ and $p(x)$ are known from the previous step. $N_D(x)$ is initially assumed to be uniformly distributed across the length, i.e. $N_D(x) = N_D^*$. But, for later iterations, I used $N_D(x)$ got from the continuity equation that is described in the subsequent steps. One important thing to note here is that, I assumed the boundary conditions at end poins to be zero, i.e. $\phi(0) = \phi(L) = 0$. Unfortunately, due to convergence issues, I approximated $\phi(x)$ to be $\phi(x) \approx \phi_n(x) - \phi_p(x)$ for the remaining simulation, thereby, avoiding the need to solve for equation 3. So, I got the following plot for $\phi(x)$ for different values of input voltages:

3.3 Step 3:

Now, using equation 4 and boundary condition described in equation 8, I got the new values of $N_D(x)$ at end points or boundary points, i.e. $N_D(0)$and $N_D(L)$. I would be using the $\phi(x)$ got from the previous step for this.

Figure 5: Electrostatic potential - $\phi(x)/v_0$ for different input voltages (where $v_0 = 26mV$ is the thermal voltage)

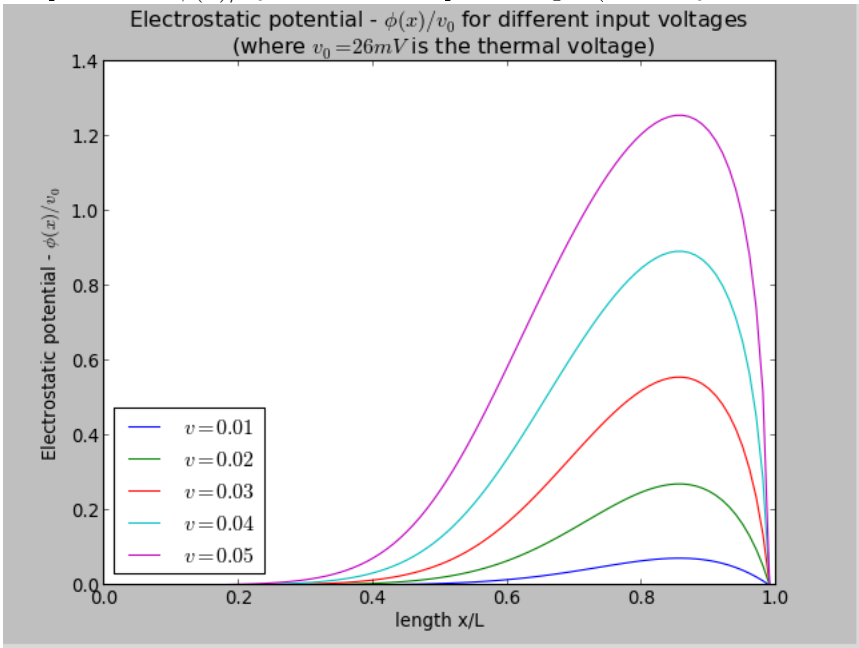

3.4 Step 4:

Finally, the new $N_D(x)$ for all other values of x, is determined using equation 5 (continuity equation) and older values of $N_D(x)$ and $\phi(x)$ which were got from the previous steps. The variation in the distribution $N_D(x)$ with time shows us the movement of the thin wall region. The exact finite difference equation that I used is derived as follows:

Combining equations (4) and (5), gives:

$$\frac{\partial}{\partial t}\left(N_D(x)\right) = D_i \frac{\partial^2}{\partial x^2}\left(N_D(x)\right) + \mu_i \left[\frac{\partial}{\partial x}\left(N_D(x)\right)\right]\left[\frac{\partial \phi(x)}{\partial x}\right] + \mu_i N_D(x) \frac{\partial^2 \phi(x)}{\partial x^2}$$

This could be written in finite difference form as folows:

$$\frac{N_D^{new}(x) - N_D^{old}(x)}{\Delta t} = D_i \frac{N_D^{old}(x+h) - 2N_D^{old}(x) + N_D^{old}(x-h)}{h^2} + \mu_i \left[\frac{N_D^{old}(x+h) - N_D^{old}(x-h)}{2h}\right]\left[\frac{\phi(x+h) - \phi(x-h)}{2h}\right] + \mu$$

The $N_D^{new}(x)$ got from the above equation was assumed to be $N_D^{old}(x)$ and the above equation was solved again. This iteration was repeated until a steady state $N_D(x)$ was got. That is, when the left hand side of equation (5) almost goes to zero. This actually, results in constant $J_{ION}(x)$ for all x, because its gradient becomes zero. But, from the boundary equation (8), we know that this constant should be zero. The steady state $N_D(x)$ for the ions is plotted in the following diagram. Here, $N_D(x)$, was initially assumed to be constant everywhere, which was $N_D^* = 5 \times 10^{19} cm^{-3}$.

Figure 6: Semi-log plot of Ionic concentration - $N_D(x)/N_D^*$

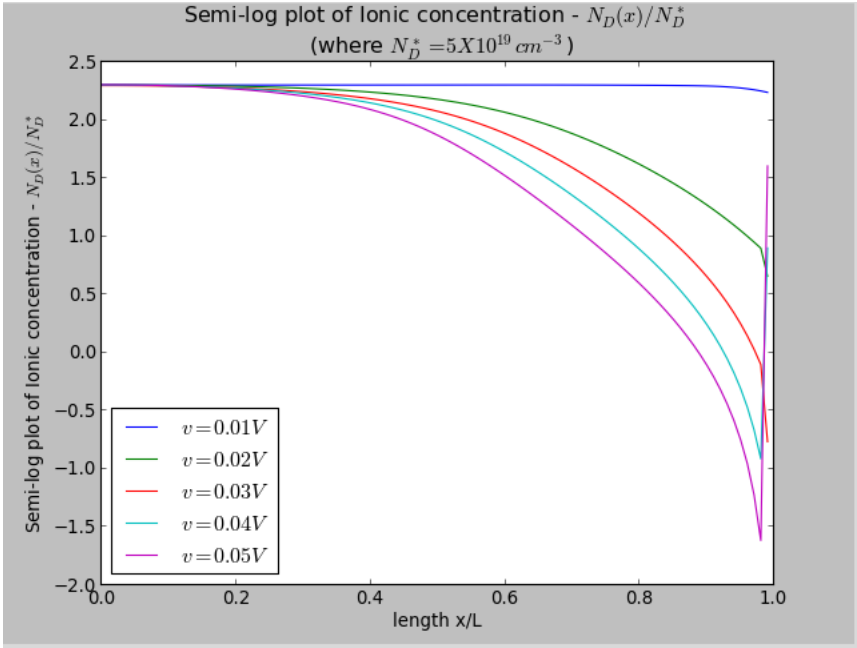

Step 1 was repeated iteratively for a particular voltage value, until steady state condition was reached. This was done separately for electrons and holes. Then, from step 2, $\phi(x)$ was found. This was assumed to be constant for all the time instants. Then, to get the values of $N_D(x)$, for next time instant, i.e. for $t + \triangle t$, where $\triangle t$ is the time step in this simulation, step 3 and 4 are performed using the values of $N_D(x)$ at time t and $\phi(x)$. This gave $N_D(x)$ for time $t + \triangle t$. This was repeated iteratively until $N_D(x)$ reaches a steady state. The above plot shows that these steady state $N_D(x)$ moves inside as the voltage is increased. Thus, the movement of thin wall region in the TiO_2 memristor as the voltage is varied is shown, thereby verifying the memristive action in such a device.

References

[1] D. B. Strukov, G. S. Snider, D. R. Stewart, R. S. Williams, Nature 2008, 453, 80.

[2] L. O. Chua, IEEE Trans. Circuit Theory 1971, 18, 507.

[3] L. O. Chua, S. M. Kang, Proc. IEEE 1976, 64, 209.

[4] D. B. Strukov, J. L. Borghetti, D. R. Stewart, R. S. Williams, 2009. Small, 5: 1058–1063.